Billion Years of Evolution on Earth (Princeton Univ. Press, Princeton, NJ, 2003).
4. S. Xiao, Y. Zhang, A. H. Knoll, *Nature* **391**, 553 (1998).
5. M. A. Fedonkin, in *The Vendian System*, B. S. Sokolov, A. B. Iwanowski, Eds. (Springer-Verlag, Heidelberg, 1990), vol. 1, pp. 132–137.
6. R. J. F. Jenkins, *Precambrian Res.* **73**, 51 (1995).
7. M. E. Clapham, G. M. Narbonne, *Geology* **30**, 627 (2002).
8. M. E. Clapham, G. M. Narbonne, J. G. Gehling, *Paleobiology* **29**, 527 (2003).
9. T. D. Ford, *Proc. Yorks. Geol. Soc.* **31**, 211 (1958).
10. A. Yu. Zhuravlev, *Neues Jahrb. Geol. Palaeontol. Abh.* **190**, 299 (1993).
11. K. J. Peterson, B. M. Waggoner, J. W. Hagadorn, *Integr. Comp. Biol.* **43**, 127 (2003).
12. A. Seilacher, *J. Geol. Soc. (London)* **149**, 607 (1992).
13. M. W. Martin *et al.*, *Science* **288**, 841 (2000).
14. S. A. Bowring, P. M. Myrow, E. Landing, J. Ramenzani, *NASA Astrobiology Unit, General Meeting 2003*, Abstract 13045 (http://nai.arc.nasa.gov/institute/general_meeting_2003/AbstractBook.pdf).
15. G. M. Narbonne, J. G. Gehling, *Geology* **31**, 27 (2003).
16. J. G. Gehling, *Mem. Geol. Soc. India* **20**, 181 (1991).
17. J. G. Gehling, J. K. Rigby, *J. Paleontol.* **70**, 185 (1996).
18. M. A. Fedonkin, B. M. Waggoner, *Nature* **388**, 868 (1997).
19. A. Seilacher, *Palaios* **14**, 86 (1999).
20. D. A. Wood, R. W. Dalrymple, G. M. Narbonne, J. G. Gehling, M. E. Clapham, *Can. J. Earth Sci.* **40**, 1375 (2003).
21. G. M. Narbonne, R. W. Dalrymple, J. G. Gehling, *Geol. Assoc. Can. Field Guide B5* (2001).
22. S. B. Misra, *Geol. Soc. Am. Bull.* **80**, 2133 (1969).
23. M. M. Anderson, S. Conway Morris, *Proceedings of the Third North American Paleontological Convention* (Montreal, August 1982), vol. 1, part 1, pp. 1–8.
24. J. G. Gehling, *Palaios* **14**, 40 (1999).
25. R. J. F. Jenkins, *Paleobiology* **11**, 336 (1985).
26. J. Dzik, *J. Morphol.* **252**, 315 (2002).
27. D. Grazhdankin, *Paleobiology* **30**, 203 (2004).
28. Systematic paleontology will be presented elsewhere.
29. H. Boynton, T. D. Ford, *Mercian Geol.* **13**, 165 (1995).
30. Supported by a Natural Sciences and Engineering Research Council of Canada (NSERC) Discovery Grant. A. Daley, A. Ichaso, and R. W. Dalrymple contributed to the discovery and documentation of this fossil bed. C. Greentree, M. Mussa-Caleca, P. Pufahl, and M. Laflamme assisted with manuscript preparation. J. G. Gehling, R. W. Dalrymple, and M. Laflamme reviewed the manuscript.

28 April 2004; accepted 30 June 2004
Published online 15 July 2004;
10.1126/science.1099727
Include this information when citing this paper.

Intracellular Acidosis Enhances the Excitability of Working Muscle

Thomas H. Pedersen,[1] Ole B. Nielsen,[1] Graham D. Lamb,[2] D. George Stephenson[2]*

Intracellular acidification of skeletal muscles is commonly thought to contribute to muscle fatigue. However, intracellular acidosis also acts to preserve muscle excitability when muscles become depolarized, which occurs with working muscles. Here, we show that this process may be mediated by decreased chloride permeability, which enables action potentials to still be propagated along the internal network of tubules in a muscle fiber (the T system) despite muscle depolarization. These results implicate chloride ion channels in muscle function and emphasize that intracellular acidosis of muscle has protective effects during muscle fatigue.

Contraction in a twitch skeletal muscle fiber in response to a nerve impulse is the result of a complex series of events known as excitation-contraction-coupling (*1*) (ECC). ECC consists of (Fig. 1) (i) initiation and propagation of an action potential (AP) along the surface membrane and into the T system, (ii) activation of the voltage sensors (VSs) in the tubular wall, (iii) signal transmission to the sarcoplasmic reticulum (SR) from which the activator ion Ca^{2+} is released, and (iv) activation by Ca^{2+} of the Ca^{2+}-regulatory system associated with the contractile apparatus. Intense muscle activity leads to a decline in mechanical performance (power output, force, and velocity of shortening), which is generally known as muscle fatigue (*1–4*). Intracellular acidification of the working muscle associated with the production of lactic acid has been said to contribute to muscle fatigue (*2*). This is because intracellular acidification reduces the sensitivity of the contractile apparatus to Ca^{2+} and, under some circumstances, the maximum Ca^{2+}-activated force that is generated (*2*). However, the adverse actions of intracellular pH are not as great as originally thought (*5*, *6*). Another factor in muscle fatigue is reduced ability of the T system to conduct APs as a result of excitation-induced accumulation of K^+ in the T system (*3*, *4*). The accumulation of K^+ causes depolarization, which inactivates the

[1]Department of Physiology, University of Aarhus, DK-8000, Denmark. [2]Department of Zoology, La Trobe University, Bundoora, Melbourne, Victoria, 3086, Australia.

*To whom correspondence should be addressed. E-mail: G.Stephenson@zoo.latrobe.edu.au

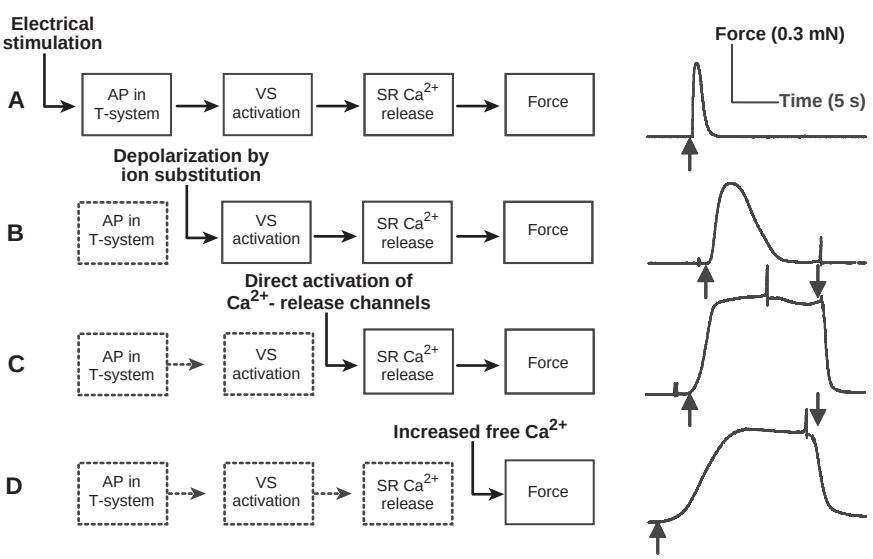

Fig. 1. Modes of activation of mechanically skinned muscle fibers. The force responses (right) were all obtained with the same preparation. Calibration bars for all force responses: vertical, 0.3 mN, and horizontal, 5 s. Upward-pointing arrows indicate time of activation and downward-pointing arrows indicate subsequent relaxation in a heavily buffered EGTA solution ($[Ca^{2+}] < 1$ nM). (**A**) Electrical stimulation initiates APs in the sealed T system. Shown is a tetanic contraction at 25 Hz stimulation with square pulses of 2-ms duration for 1s and field strength of 70 V/cm in a standard K-hexamethylene-diamine-tetraacetate (K-HDTA) solution with Cl^- (*10*, *11*, *21*). (**B**) Depolarization of the T system (by replacing all K^+ in the solution with Na^+) activates VSs independently of APs in the T system. The force response resulted from transfer of the preparation from a standard K-HDTA solution to depolarizing Na-HDTA solution (*5*). (**C**) Direct activation of SR Ca^{2+}-release channels, causing Ca^{2+} release from the SR, and force production when free $[Mg^{2+}]$ in the solutions was lowered from 1 mM to 0.015 mM (*5*). (**D**) Direct activation of the contractile apparatus in Ca^{2+}-buffered solutions (*5*, *10*, *11*, *21*). The preparation was transferred from the standard K-HDTA solution ($[Ca^{2+}] = 100$ nM) to heavily buffered Ca-EGTA solution ($[Ca^{2+}] = 30$ μM).

Na^+ channels responsible for the generation and propagation of APs (*3*, *7*). Unexpectedly, the loss of muscle excitability and force seen in depolarized muscles is greatly counteracted by intracellular acidification (*8*), although the underlying mechanism is not understood.

In this study, we used a muscle fiber preparation from the extensor digitorum longus (EDL) muscle of the rat in which the surface membrane is removed by microdissection, causing the T system to seal off and all steps in ECC to be maintained (*5*, *9*–*11*). This preparation allows direct access to the intracellular environment, thus permitting separate control of the intracellular pH and T system membrane potential. Such mechanically skinned muscle fibers can be activated at any individual step in the ECC process (i) by electrical stimulation that triggers APs in the T system (*10*, *11*), (ii) by direct activation of the VSs in the T system (*5*), (iii) by directly releasing Ca^{2+} from the SR (*5*), or (iv) by directly activating the contractile apparatus in Ca^{2+}-buffered solutions (*5*, *10*) (Fig. 1). Thus, it is possible to determine the separate and the combined effects of T system depolarization and intracellular acidification on T system excitability (that is, generation and propagation of APs in the T system) and to assess likely effects on muscle fatigue.

If the potential across the T system is reduced for a sustained period, a proportion of the VSs become dysfunctional (inactivated). This was achieved here by equilibrating the skinned fibers in solutions with decreased myoplasmic (intracellular) K^+ concentration ($[K^+]_i$) at constant $[K^+]_i[Cl^-]_i$ product ($[Cl^-]_i$ is the concentration of Cl^-) (*12*). The remaining (noninactivated) VSs were then activated by fully depolarizing the T system with application of a solution with all K^+ removed (Fig. 2A). The force responses to full depolarization were then plotted against the $[K^+]_i$ in the various equilibration solutions to show the inactivation behavior of the VSs. Because the inactivation curves of the VSs (Fig. 2B) at pH = 6.6 and pH = 7.1 were virtually the same, we conclude that the ECC steps starting from VS activation up to the activation of the contractile apparatus (Fig. 1) are largely unaffected by intracellular acidification. This is consistent with inactivation of VSs being unaffected by intracellular acidosis (*13*). The overlap of the two curves in Fig. 2B also confirms that the membrane potential across the T system at any given $[K^+]_i$ was essentially the same at pH values of 7.1 and 6.6. The values of membrane potential for the various $[K^+]_i$ were calculated from the Goldman-Hodgkin-Katz equation (*14*), assuming 4 mM for K^+ and 150 mM for Na^+ in the lumen of the sealed T system, relative permeability for K^+ as compared to Na^+ of 100:1, and passive distribution of Cl^- across the T system. In contrast, force responses to APs in the T system elicited by electrical stimulation (*10*, *11*) did display pH dependence (Fig. 2, C and D) (preparations were tetanically stimulated at 25 Hz at pH = 7.1 and at pH = 6.6). When the T system was moderately depolarized at $[K^+]_i$ values of 75 and 60 mM, there was a significantly greater loss of tetanic force at pH = 7.1 than at pH = 6.6 ($P < 0.05$, $n = 10$). The loss in force response with AP stimulation occurred at more negative potentials than did VS inactivation (compare Fig. 2D with Fig. 2B), showing that the force loss was due predominantly to AP failure rather than inadequate VS activation. These results indicate that intracellular acidosis protects against the loss of force caused by depolarization when activation is initiated by APs, as occurs in vivo, and

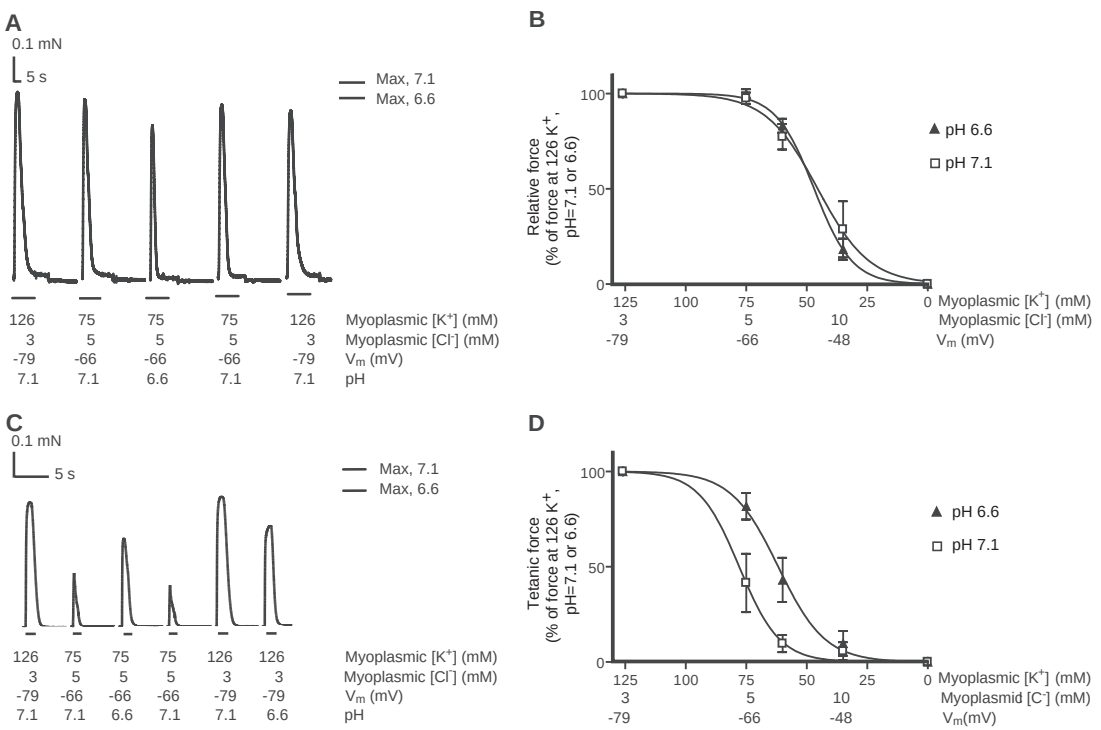

Fig. 2. Effect of pH and T system depolarization on force responses induced by direct VS activation (**A** and **B**) or tetanic stimulation at 25 Hz (**C** and **D**) in the presence of Cl^- in mechanically skinned fibers at 25° ± 2°C. EDL muscles of rats [Long Evans Hooded, 6-month-old males, killed by halothane overdose (*5*)] were placed in paraffin oil and skinned fibers were prepared as described (*5*, *10*, *11*, *21*) . Fibers were attached to a sensitive force transducer and bathed in solutions mimicking the myoplasmic environment (*5*, *10*, *11*, *21*). The K-HDTA standard solution at pH = 7.10 contained 126 mM K^+, 17 mM methylsulfate, 3 mM Cl^-, 40 mM Na^+, 40 mM $HDTA^{2-}$, 1 mM Mg^{2+} (free), 8 mM adenosine triphosphate, 10 mM creatine phosphate, 90 mM Hepes buffer, 0.05 mM Bapta [(1,2-bis*0*-aminophenoxy)ethane-*N*,*N*,*N*′,*N*′-tetraacetic acid], and 100 nM Ca^{2+}. The K-HDTA standard solution at pH = 6.60 was identical to the K-HDTA solution at pH = 7.10 with respect to all ions except that it contained 9 mM Pipes and Hepes was reduced to 80 mM to maintain osmotic balance (295 ± 2 mmol/kg). In solutions with decreased $[K^+]_i$, K^+ was replaced with NH_4^+ and methylsulfate with Cl^- to maintain constant $[K^+]_i[Cl^-]_i$ product. (A and C) Representative force traces from two individual fibers. Bars under traces represent the duration of stimulation [ion substitution for (A) and 25-Hz tetanic stimulation for (C)]. The voltage sensor–activated force response at pH = 6.6 (75 mM K^+) is only slightly smaller than the corresponding response at pH = 7.1, with the difference entirely due to the decrease in maximum Ca^{2+}-activated force at pH = 6.6, which was smaller by 19 ± 9% ($n = 49$) compared with that at pH = 7.1. The horizontal lines in (A) and (C) indicate the maximum Ca^{2+}-activated force generated at pH = 7.1 and pH = 6.6 in buffered Ca-EGTA solutions ($[Ca^{2+}] = 30$ μM) in which $HDTA^{2-}$ was replaced by $Ca\text{-}EGTA^{2-}$. Calibration bars: vertical, 0.1 mN, and horizontal, 5 s. Membrane potential in the various $[K^+]_i$ solutions was calculated from the Goldman-Hodgkin-Katz equation (*14*). For each data point *n* was from 5 to 8.

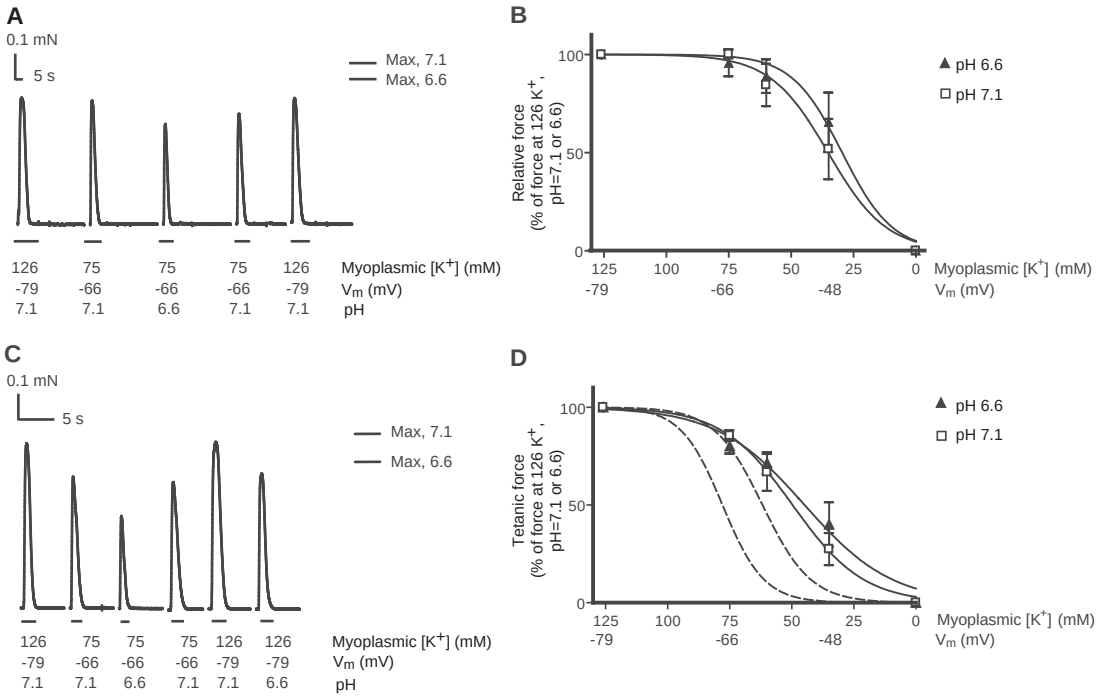

Fig. 3. Effect of pH and T system depolarization on force responses at 25° ± 2°C induced by direct VS activation (**A** and **B**) or tetanic stimulation at 25 Hz (**C** and **D**) in the absence of Cl^-. Before skinning, the muscles were equilibrated for 30 min in Cl^--free Ringer's solution containing 65 mM Hepes, 1.2 mM Ca^{2+}, 115 mM sodium methylsulfate, 4 mM K^+, 1.2 mM phosphate, and 5 mM glucose. NaOH was used to bring pH to 7.4. All intracellular solutions had the same composition as the solutions described in the legend of Fig. 2 except Cl^- was replaced with methylsulfate. Membrane potential in the various $[K^+]_i$ solutions was calculated as described (Fig. 2). (A and C) Representative force traces from two individual fibers. Bars under traces represent the duration of stimulation. (C) The horizontal lines indicate the maximum Ca^{2+}-activated force at pH values of 7.1 and 6.6 in heavily buffered Ca-EGTA solutions (Fig. 2). Calibration bars: vertical 0.1 mN, horizontal 5 s. The broken lines shown in (D) represent the curves from Fig. 2D.

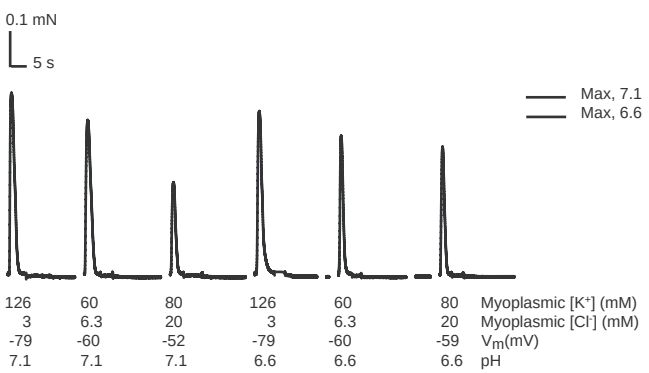

Fig. 4. Effect of pH on Cl^- permeability in the T system. Representative VS activated force responses in a mechanically skinned fiber equilibrated in solutions of different $[K^+]_i$ and $[Cl^-]_i$ at pH values of 7.1 and 6.6. Calibration bars: vertical, 0.1 mN; horizontal, 5 s. At constant $[K^+]_i[Cl]_i$ product, the membrane potentials were calculated as described in text, and at 80 K^+ and 20 Cl^- the membrane potential was estimated from Fig. 2B.

indicate that this protective effect may be due to enhanced excitability of the T system.

In rested muscle, Cl^- is the most membrane-permeant ion (*15*–*18*). The high membrane permeability to Cl^- at normal pH stabilizes the resting membrane potential, but the cost of this is that a comparatively large inward Na^+ current is needed to sustain a propagating AP (*16*, *18*). Because lowering pH reduces Cl^- conductance (*19*, *20*), we examined whether Cl^- plays a role in the protective effect of acidity. When experiments like those in Fig. 2, A to D, were repeated without Cl^- in the myoplasm and T system, the inactivation curve for tetanic stimulation at pH = 6.6 was no different from that at pH = 7.1 (Fig. 3, C and D). Compared with the inactivation curves in the presence of C1 (indicated with broken lines in Fig. 3D), both inactivation curves were shifted to the right (to lower $[K^+]_i$ and greater depolarization) but with a greater shift at pH = 7.1 than at pH = 6.6 (Fig. 3D). Thus, the pH effect seen in Fig. 2D is associated with the presence of Cl^-.

To evaluate whether intracellular acidosis decreases the Cl^- permeability of the T system, we did an experiment in which preparations were activated by ion substitution after equilibration in a solution with 80 mM K^+ and 20 mM Cl^-, which is about four times the $[Cl^-]_i$ needed to keep the $[K^+]_i[Cl^-]_i$ constant (Fig. 4). Under these conditions, Cl^- will tend to depolarize the T system more than the reduction in K^+ concentration would, and a high Cl^- permeability would therefore increase the level of chronic depolarization. Consequently the force response to maximal VS activation was expected to be reduced. The drop in force at 80 mM K^+ and 20 mM Cl^- was larger at pH = 7.1 than at pH = 6.6. From the inactivation curves in Fig. 2B, the membrane potential of the T system at 80 mM K^+ and 20 mM Cl^- was estimated to be –52 mV at pH = 7.1 and –59 mV at pH = 6.6 (*n* from 7 to 10). On the basis of the Goldman-Hodgkin-Katz equation, this change in membrane potential showed that the permeability of Cl^- in the T system was reduced by around 74% at pH = 6.6 compared to that at pH = 7.1. The fact that at pH = 6.6 the T system Cl^- permeability was not completely abolished may explain why the inactivation curve for tetanic stimulation at pH = 6.6 was not shifted as much as the inactivation curves were when Cl^- was totally removed (Fig. 3D).

We find that, in the presence of Cl^-, intracellular acidosis increases the excitability of the T system in depolarized muscles fibers, thus counteracting fatigue at a critical step in ECC. In this model of working muscle, acidic pH reduced Cl^- permeability, thereby reducing the size of the Na^+ current needed to generate a propagating AP. Thus, down-regulation of T system Cl^- permeability by intracellular acidosis is important for preserving a fully operational T system in working muscle.

References and Notes

1. D. G. Stephenson, G. D. Lamb, G. M. Stephenson, *Acta Physiol. Scand.* **162**, 229 (1998).
2. R. H. Fitts, *Physiol. Rev.* **74**, 49 (1994).
3. G. Sjøgaard, *Acta Physiol. Scand. Suppl.* **593**, 1 (1990).
4. O. M. Sejersted, G. Sjøgaard, *Physiol. Rev.* **80**, 1411 (2000).
5. G. D. Lamb, D. G. Stephenson, *J. Physiol.* **478**, 331 (1994).
6. H. Westerblad, D. G. Allen, J. Lännergren, *News Physiol. Sci.* **17**, 17 (2002).
7. R. L. Ruff, *Acta Physiol. Scand.* **156**, 159 (1996).

8. O. B. Nielsen, F. de Paoli, K. Overgaard, *J. Physiol.* **536**, 161 (2001).
9. B. S. Launikonis, D. G. Stephenson, *J. Gen. Physiol.* **123**, 231 (2004).
10. G. S. Posterino, G. D. Lamb, D. G. Stephenson, *J. Physiol.* **527**, 131 (2000).
11. G. S. Posterino, T. L. Dutka, G. D. Lamb, *Pflugers Arch.* **442**, 197 (2001).
12. A. L. Hodgkin, P. Horowitz, *J. Physiol.* **148**, 127 (1959).
13. E. M. Balog, R. H. Fitts, *J. Appl. Physiol.* **90**, 228 (2001).
14. B. Hille, *Ion Channels of Excitable Membranes* (Sinauer, Sunderland, MA, ed. 3, 2001).
15. A. F. Dulhunty, *J. Membr. Biol.* **45**, 293 (1979).
16. A. H. Bretag, *Physiol. Rev.* **67**, 618 (1987).
17. J. R. Coonan, G. D. Lamb, *J. Physiol.* **509**, 551 (1998).
18. T. J. Jentsch, V. Stein, F. Weinreich, A. A. Zdebik, *Physiol. Rev.* **82**, 503 (2002).
19. O. F. Hutter, A. E. Warner, *J. Physiol.* **189**, 403 (1967).
20. P. T. Palade, R. L. Barchi, *J. Gen. Physiol.* **69**, 325 (1977).
21. N. Ørtenblad, D. G. Stephenson, *J. Physiol.* **548**, 139 (2003).
22. This research was supported by the Danish Medical Research Council (22-02-0188), University of Aarhus, Australian Research Council, and National Health and Medical Research Council of Australia.

7 June 2004; accepted 27 July 2004

Local Nanomechanical Motion of the Cell Wall of *Saccharomyces cerevisiae*

Andrew E. Pelling, Sadaf Sehati, Edith B. Gralla, Joan S. Valentine, James K. Gimzewski*

We demonstrate that the cell wall of living *Saccharomyces cerevisiae* (baker's yeast) exhibits local temperature-dependent nanomechanical motion at characteristic frequencies. The periodic motions in the range of 0.8 to 1.6 kHz with amplitudes of ~3 nm were measured using the cantilever of an atomic force microscope (AFM). Exposure of the cells to a metabolic inhibitor causes the periodic motion to cease. From the strong frequency dependence on temperature, we derive an activation energy of 58 kJ/mol, which is consistent with the cell's metabolism involving molecular motors such as kinesin, dynein, and myosin. The magnitude of the forces observed (~10 nN) suggests concerted nanomechanical activity is operative in the cell.

Many biological processes taking place inside the living cell rely on the nanomechanical properties of cellular substructures and the cell membrane or wall itself. The atomic force microscope (AFM) (*1*) yields information on the integrity and local nanomechanical properties of mammalian and microbial cellular membranes under normal and stressed metabolic conditions (*2*–*11*). The sensitivity and ability to apply only minimal forces on a cell makes the AFM a useful nondestructive tool to study cellular nanomechanics. AFM has also been used to measure the natural beating motion in the 0.05 to 0.4 Hz range of cardiomyocytes (heart cells), which is a property related to the cell's physiology (*3*, *12*). In a low-noise environment, the AFM has the sensitivity to measure local nanoscale motion of cells. Here, we have used this capability to discover distinct periodic nanomechanical motion of yeast cells, which we relate to metabolic processes within the cell.

In a typical image of a dense layer of yeast cells air dried onto a mica surface (Fig. 1), yeast

Department of Chemistry and Biochemistry, University of California, Los Angeles, 607 Charles E. Young Drive East, Los Angeles, CA 90095, USA.

*To whom correspondence should be addressed. E-mail: gim@chem.ucla.edu.

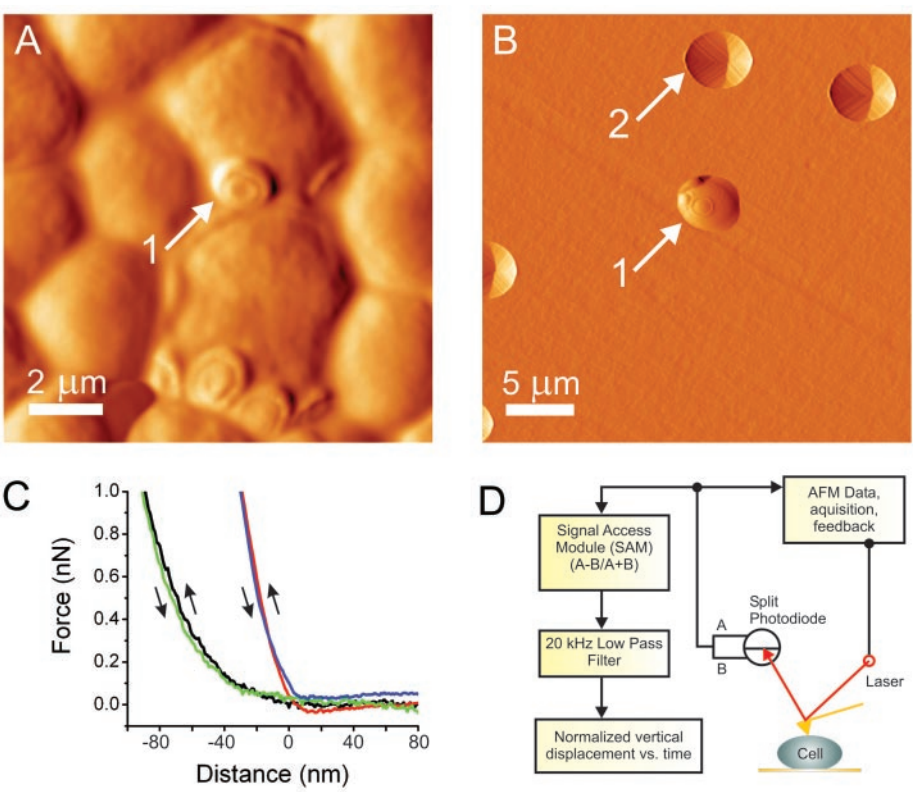

Fig. 1. Typical deflection mode images of yeast cells are shown in (**A** and **B**) [the color scale bar in (A) corresponds to deflections between 0 to 320 nm and 0 to 120 nm in (B)]. A dense layer of yeast cells dried onto mica and imaged in air is shown in (A). Yeast cells are about 5 μm in diameter and often have bud scars on the cell surface (arrow 1). Mechanical trapping is used to study live cells in YPD medium at 30°C. In (B), a typical image of a living yeast cell (arrow 1) trapped in a 5-μm filter pore is shown [empty pores (arrow 2) are easily distinguishable from trapped cells in the image]. Force-distance curves (**C**) can be obtained by monitoring the deflection of the cantilever as it is extended (up arrow) and retracted (down arrow) from the cell in order to measure the local cellular nanomechanical properties. The zero point on the displacement scale represents the point where the AFM tip first comes into contact with the cell. A force-distance curve on the cell body (black line, extension; and green line, retraction) and the bud scar (blue line, extension; and red line, retraction) are shown. Local nanomechanical spring constants (k_{cell}) can be determined from the slope of the linear portion of the curves. Bud scars always display higher k_{cell} because of the increased chitin content of the area (*8*). A schematic of the experimental setup (**D**) outlines the process of measuring the local nanomechanical motion of the cell wall. The AFM cantilever is positioned on top of a living cell, and the scan size is set to 0 nm. The deflection of the cantilever is measured with a photodiode. The signal is acquired with a breakout box (SAM, signal access module), low-pass filtered (20 kHz), and sampled using another computer at 40 kHz.

Intracellular Acidosis Enhances the Excitability of Working Muscle

Thomas H. Pedersen *et al.*

Science **305**, 1144 (2004);
DOI: 10.1126/science.1101141